Geophysical Research Letters

RESEARCH LETTER
10.1029/2022GL100271

Statistical Downscaling of Seasonal Forecasts of Sea Level Anomalies for U.S. Coasts

Xiaoyu Long[1,2], **Sang-Ik Shin**[1,2], **and Matthew Newman**[2]

[1]CIRES, University of Colorado Boulder, Boulder, CO, USA, [2]NOAA Physical Sciences Laboratory, Boulder, CO, USA

Key Points:

- Sea level prediction from relatively coarse operational forecasts can be enhanced to finer coastal scales using statistical downscaling
- Downscaling can be determined by multivariate linear regression trained from high-resolution reanalysis and its coarse-grained counterpart
- This downscaling method significantly improves skill compared to bilinearly interpolated hindcasts at several U.S. tide gauge locations

Supporting Information:

Supporting Information may be found in the online version of this article.

Correspondence to:

X. Long,
xiaoyu.long@noaa.gov

Citation:

Long, X., Shin, S.-I., & Newman, M. (2023). Statistical downscaling of seasonal forecasts of sea level anomalies for U.S. coasts. *Geophysical Research Letters*, *50*, e2022GL100271. https://doi.org/10.1029/2022GL100271

Received 30 JUN 2022
Accepted 3 FEB 2023

Author Contributions:

Conceptualization: Xiaoyu Long, Sang-Ik Shin, Matthew Newman
Funding acquisition: Matthew Newman
Methodology: Xiaoyu Long, Sang-Ik Shin, Matthew Newman
Project Administration: Matthew Newman
Supervision: Sang-Ik Shin, Matthew Newman
Visualization: Xiaoyu Long
Writing – original draft: Xiaoyu Long, Sang-Ik Shin, Matthew Newman
Writing – review & editing: Xiaoyu Long, Sang-Ik Shin, Matthew Newman

Abstract Increasing coastal inundation risk in a warming climate will require accurate and reliable seasonal forecasts of sea level anomalies at fine spatial scales. In this study, we explore statistical downscaling of monthly hindcasts from six current seasonal prediction systems to provide a high-resolution prediction of sea level anomalies along the North American coast, including at several tide gauge stations. This involves applying a seasonally invariant downscaling operator, constructing by linearly regressing high-resolution (1/12°) ocean reanalysis data against its coarse-grained (1°) counterpart, to each hindcast ensemble member for the period 1982–2011. The resulting high-resolution coastal hindcasts have significantly more deterministic skill than the original hindcasts interpolated onto the high-resolution grid. Most of this improvement occurs during summer and fall, without impacting the seasonality of skill noted in previous studies. Analysis of the downscaling operator reveals that it boosts skill by amplifying the most predictable patterns while damping the less predictable patterns.

Plain Language Summary Currently, the large computer models that form the basis of seasonal climate prediction systems produce coastal sea level forecasts spaced about 100 km apart. This is too coarse to meet the needs of U.S. coastal ocean management and services, which are becoming increasingly important as sea levels rise in a warming climate. In this study, we explored a method to provide such information on much smaller spatial scales, which better correspond to local coastal sea level measurements by tide gauges. We developed an efficient way to generate monthly sea level predictions on distances as small as 10 km apart, by applying the observed statistical relationship between sea level variations on scales of 100–1,000 km and finer-scale coastal ocean observations to the original coarser model predictions. By testing our approach on past forecasts ("hindcasts") from existing climate forecast systems, we found that we could improve forecasts for different local regions along both the U.S. West and East Coasts.

1. Introduction

Sea level rise has increased the frequency, severity, and duration of coastal flooding in the past few decades (Ezer & Atkinson, 2014; Moftakhari et al., 2015; Sweet et al., 2014; Wdowinski et al., 2016). These changes can impact coastal communities through groundwater inundation (Rotzoll & Fletcher, 2013), beach erosion (Anderson et al., 2015) and storm-drain backflow and damage to the infrastructure (Habel et al., 2020). Coastal flooding frequency, due both to accelerated sea level rise (Nerem et al., 2018; Sallenger et al., 2012) and increasing sea level variability under climate change (Widlansky et al., 2020), is projected to steadily increase (Dahl et al., 2017; Kriebel et al., 2015; Kruel, 2016; Thompson et al., 2021; Wdowinski et al., 2016) and double by 2050 (Vitousek et al., 2017). This increasing risk to coastal infrastructure necessitates more accurate and reliable prediction of high-water level events months and seasons in advance.

Previous studies have demonstrated that dynamical seasonal forecasting systems can forecast sea level variations in the open ocean and at some coastal locations (Long et al., 2021; McIntosh et al., 2015; Miles et al., 2014; Widlansky et al., 2017), but in general coastal prediction remains challenging. First, by definition, the coasts are the numerical boundary of the ocean model, requiring special treatment in numerical integration. Second, the current generation of forecast systems has spatial resolution too coarse to fully resolve the topography and fine-scale dynamics near the coasts. This issue could be addressed with much finer grid spacing in global forecast models, but the resulting computational burden and model output storage requirements would be considerable, especially given the need for multiple ensemble members.

Alternatively, using downscaling techniques (Castro et al., 2005; Heyen et al., 1996; Pielke Sr & Wilby, 2012; Sithara et al., 2022), regional forecast output with higher resolution than the original coarse-grained forecasts

can be obtained either dynamically, through regional numerical models with higher resolution but more limited domain, or statistically, through statistical relationships between coarse-grained and fine-scale data. Dynamical downscaling can potentially benefit from the regional model's better resolved dynamics and topography (M. A. Alexander et al., 2020; Shin & Alexander, 2020), but still requires substantial computational and storage resources. Statistical downscaling, on the other hand, usually provides comparable results without lengthy numerical integration and often benchmarks the evaluation of dynamic downscaling (Goubanova et al., 2011).

This study aims to develop high-resolution forecasts of coastal sea level anomalies from existing seasonal forecast products, using simple regression-based statistical downscaling whose results can serve to benchmark the future development of more advanced downscaling methods. This paper is organized as follows. Section 2 introduces the observational and reanalysis data and model hindcast data set used in this study. Section 3 describes the details of the regression-based downscaling procedure. The validation of the downscaling technique and the deterministic skill of the downscaled hindcasts are presented in Section 4. Section 5 includes the conclusion.

2. Data Description

In our analysis, we use monthly observations of sea level from coastal tide gauges, sea surface height (SSH) fields from reanalysis, and coupled climate model hindcast products.

2.1. Tide Gauge Observation

Six tide gauge stations (black dots in Figure 1: San Diego, San Francisco, South Beach, Virginia Key, Charleston and Atlantic City) are chosen to represent a variety of coastal locations in the United States. Tide gauge observations usually have long time coverage and are fairly consistent with other observations including satellite altimetry (Long et al., 2021).

2.2. GLORYS Reanalysis

GLORYS Ocean Reanalysis Version 12v1 (hereafter GLORYS; Jean-Michel et al., 2021) is a global eddy-resolving ocean and sea ice reanalysis, made by the Copernicus Marine Environment Monitoring Service, providing monthly ocean fields in 1/12° horizontal resolution, covering the period from 1993 to present. The reanalysis system assimilates along-track satellite derived sea level anomalies, satellite derived sea surface temperature, and in situ temperature and salinity vertical profiles, but not tide gauge data. However, extensive comparison shows that tide gauge observations are highly correlated with GLORYS SSH output along the U.S. coast (Amaya et al., 2022, and Figure S1 in Supporting Information S1), more than other reanalysis products (not shown).

2.3. Hindcasts

We downscaled hindcasts from six current generation seasonal forecast systems (Table S1 in Supporting Information S1), from different operational centers, using models with different resolution, assimilation, and parameterization schemes (Kirtman et al., 2014; Merryfield et al., 2013; Saha et al., 2014; Wedd et al., 2022; Zhang et al., 2007). SSH hindcast ensembles from each model, initialized in each month from 1982 to 2011 with lead times up to 12 months, were used in this study. We defined the lead-1 month as the same month during which the model forecast is initialized. For example, if the forecast was initialized on January 1st, then the monthly averaged forecast for January was the lead-1 month forecast (in some other studies this is called lead-0 or lead-0.5 month), February was the lead-2 month forecast, and so on. We removed the mean bias from the hindcasts, defined as the initialization month and lead-time dependent climatology determined separately for each model, as is common practice for seasonal forecasts initialized with full field variables (Smith et al., 2013; Vannitsem et al., 2018).

3. Statistical Downscaling

We determined the downscaling relationship by relating an observational fine-scale data set to a coarse-grained version of itself, which is then applied to the bias-corrected hindcasts to yield downscaled hindcasts. In such analyses, the predictor domain could differ from the predictand domain (Goubanova et al., 2011); the former is usually larger than the latter to capture large-scale variations. For the predictor, we used coarse-grained SSH

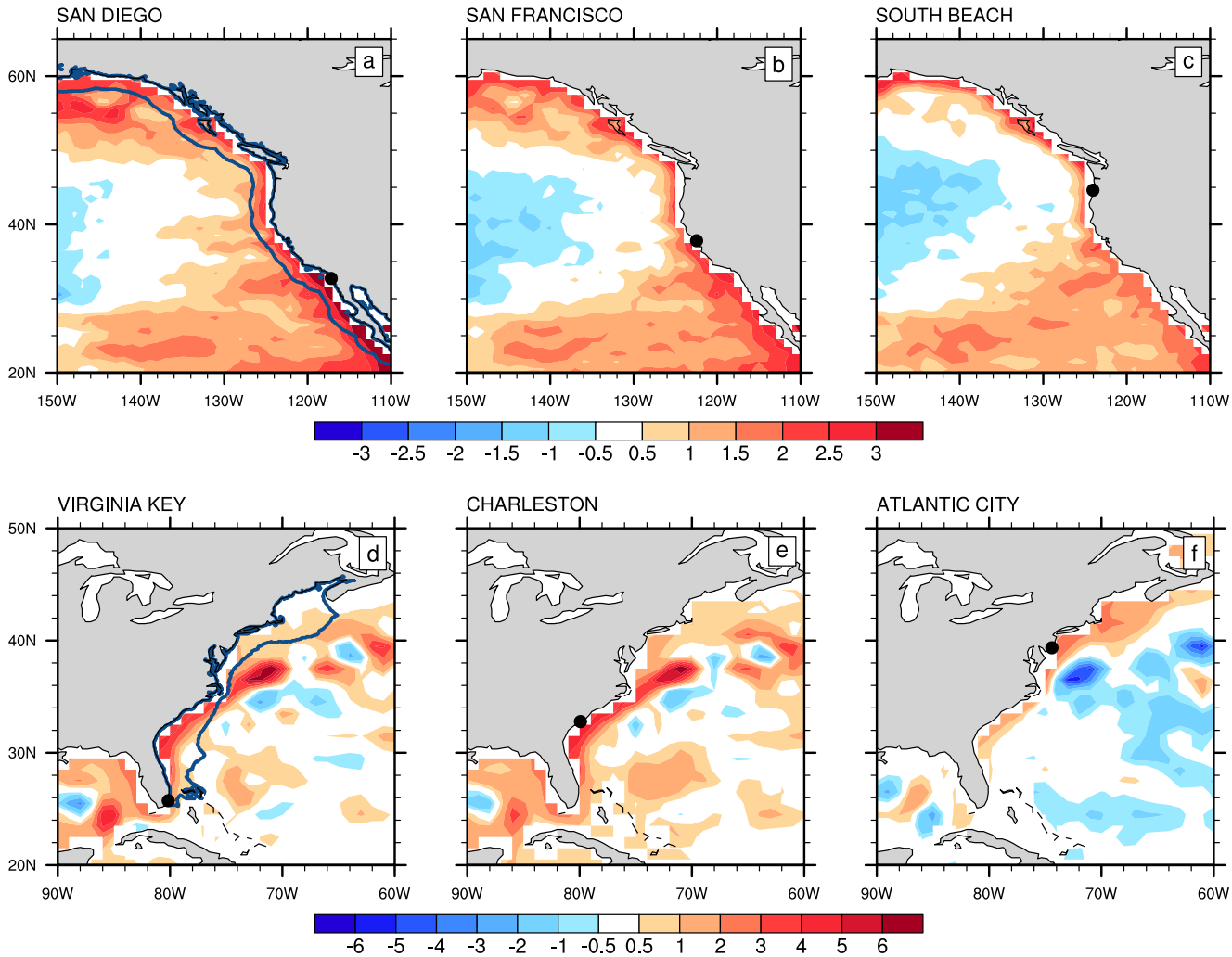

Figure 1. Regression maps of sea surface height anomalies from coarsened GLORYS reanalysis (1 × 1 grid spacing) onto each tide gauge observed sea level anomalies. The unit is centimeters. The name of each tide gauge is shown on the top of each panel. The black dots indicate the locations of the tide gauges. The blue lines in panels a and d indicate the predictand domains used in the downscaling multiple linear regressions.

anomalies determined by regridding the GLORYS reanalysis onto the climate model hindcast resolution (1° × 1°) using an areal conservative method, allowing the downscaling operator derived from the observational data sets to be directly applied to the hindcasts. For the predictand, we used GLORYS SSH anomalies on their original grid. Anomalies were defined as departures from the monthly climatology for the years 1993–2018.

3.1. Predictor and Predictand Domains

To identify a relevant geographic domain for the predictor, the coarse-grained SSH anomalies were regressed onto each of the tide gauge observed sea level anomalies (Figure 1). For the West Coast (Figures 1a–1c), coastal sea level variability is tightly confined to a narrow region along the coastline, dominated by coastally trapped Kelvin Waves (Allen, 1975) whose source can be traced back to the Tropics (Meyers et al., 1998). The sea level variability at San Diego (Figure 1a) is associated more strongly with coastal SSH signals and less with the open basin SSH pattern, as opposed to farther up the coast in South Beach (Figure 1c) where the dependence on coastal signals becomes weaker. Hence, to capture the large-scale pattern associated with coastal variability for all three representative tide gauges, the predictor domain for the West Coast was chosen to be all ocean points between 20°N–70°N and 150°W–110°W. ENSO is dynamically linked to West Coast variability, so there are also high regression values in the Tropics (not shown). However, including the ENSO region in the predictor domain turned out to be redundant since that information (e.g., the ENSO forced response) is already implicitly in the

mid-latitude domain we used. Using smaller predictor domains (e.g., extending only 10° of longitude from the coast) also yielded no improvement.

The dynamics of coastal variability for the East Coast are different from those of the West Coast. Along the Southeast U.S. Coast (Figures 1d and 1e), sea level variability is associated with the western boundary current (i.e., the Gulf Stream) and its extension. The weakly positive regression along the Gulf of Mexico indicates that part of the signal is from coastally trapped waves propagating from the southeast U.S. coast to the Gulf of Mexico (Calafat et al., 2018; Ezer, 2016; Pasquet et al., 2013). In contrast, sea level variability near the Northeast Coast (Figure 1f) appears mostly influenced by local processes (Little et al., 2019; Piecuch et al., 2018; Wang et al., 2022). The predictor domain for the East Coast was therefore bounded between 20°N–50°N and 90°W–60°W.

The West Coast predictand domain was set to be the area within 200 km of the coastline and within the larger predictor domain, while for the East Coast we adopt the Southeast and Northeast U.S. Continental Shelf Large Marine Ecosystem regions (L. M. Alexander, 1993). For the East Coast, extending the predictand domain to include the region from 35°N to 40°N and 75°W to 70°W, where high regression values (Figure 1c) correspond with the Gulf Stream Extension, slightly degraded Atlantic City skill and had little impact elsewhere.

3.2. Downscaling Procedure

Key to statistical downscaling is finding a statistical relationship between the predictors and the predictands of interest (e.g., Goubanova et al., 2011, and many references therein). Multiple linear regression (MLR) was used to determine the statistical relationship between the coarse-grained and fine-scale SSH anomalies, which were further truncated via EOF analysis to minimize the sampling uncertainty and thus reduce the effective degree of freedom (i.e., dimensionality) due to limited observational records. Here we used predictor/predictand truncation of 34/10 EOFs (77%/71% of the variance in each domain) for the West Coast, and 40/5 EOFs (80%/81%) for the East Coast, respectively. These truncations were chosen via consecutive 10-fold cross-validation, where 90% of the data was used to determine the operator, which was then used to downscale the remaining 10%; this process was cycled through 10 times for all possible permutations of predictor/predictand truncation pairs (see details in Text S1 and Figure S2 in Supporting Information S1).

Then, the MLR downscaling relationship becomes:

$$\mathbf{y} = \mathbf{B}\mathbf{x} + \epsilon \tag{1}$$

where $\mathbf{x}$ and $\mathbf{y}$ are vectors representing the principal component time series of predictor and predictand, respectively, $\mathbf{B}$ is the multivariate regression coefficient matrix (i.e., downscaling operator) and ϵ is the regression error. The MLR is performed between two spatially varying fields to account for spatial heterogeneity, and consequently $\mathbf{B}$ has nonzero off-diagonal elements. Once $\mathbf{B}$ is determined by minimizing the regression error, we use it to produce $\mathbf{Y_m}$, the downscaled hindcast in geographical space:

$$\mathbf{Y_m} = \Phi\mathbf{B}\Psi^{\intercal}\mathbf{X_m}$$

where $\mathbf{X_m}$ is the model hindcast in geographical space, and Φ and Ψ are the EOFs of $\mathbf{X}$ and $\mathbf{Y}$, respectively.

Some previous studies (Klaver et al., 2020; Soufflet et al., 2016) have suggested that the effective resolution of climate models can be larger than their nominal grid spacing, so we also tested additional grid point smoothing of both the coarse-grained predictors and the climate model hindcasts prior to computing EOFs. However, transforming into a truncated EOF space also acts as a spatial filter by efficiently capturing the resolved larger scales both in the predictor field and model output, and we found additional spatial pre-smoothing to be unnecessary.

We also tested whether our results depended upon the resolution of the GLORYS data set rather than its quality, by first smoothing the GLORYS data to match other coarser reanalyses' resolution and then using that as the "fine-scale" predictand, but this yielded poorer results.

3.3. Testing Downscaling Against Interpolation

Our statistical downscaling assumes that some fine-scale spatial coastal structures may have a large-scale component, and does not simply reflect local structures. Therefore, we hypothesize that downscaling is superior to

filling in finer grids with an interpolation technique using the information of nearby grid points only. To test whether this hypothesis is true, we compared our downscaled hindcasts to an interpolated hindcast data set, constructed by filling the grid points on continents (i.e., extrapolation) by solving a Poisson's equation on a coarse $1° \times 1°$ grid and then using bilinear interpolation to find the values on the GLORYS grid. To solve the Poisson equation, we treated the ocean grids as boundary conditions and solved the continental grids by integrating the Laplacian operator, which usually generates a smoother field than other filling methods.

4. Results

4.1. Regression Validation

We first show how well downscaling reproduced the observed fine-scale coastal SSH anomalies. Figure 2 shows that the downscaled SSH anomalies are generally an excellent match to the original GLORYS data within the West Coast domain (Figure 2a), with correlation between the two sets of anomalies mostly above 0.9, apart from areas away from the coast, especially regions with strong mesoscale eddy activity around 40°N (Stammer, 1997). Downscaled SSH anomalies are also highly correlated with GLORYS in the East Coast domain (Figure 2b). However, correlations are higher along the Southeast than the Northeast continental shelf, suggesting that the sea level variability in the former is associated with large-scale SSH variations while the latter is more influenced by local processes, consistent with the regression maps in Figure 1. Overall, the downscaling operator captured the relationship between observed coarse-grained and fine-scale SSH anomalies with reasonable accuracy for both coastal regions, despite their differing dynamics.

4.2. Forecast Skill

The patterns of skill of both downscaled and interpolated multi-model ensemble mean hindcasts are generally similar (Figures 3a and 3b). For the West Coast, skill maximized along the southwest coast, which could be attributed to coastally trapped Kelvin Waves. Low skill is found offshore around 40°N and in the Gulf of Alaska. Downscaling generally improved upon interpolated forecast skill, significantly so along the midlatitude coasts and in the Gulf of Alaska region (Figure 3c; see Supporting Information S1 for the method used to test significance). An SVD analysis of the downscaling operator (Figures S3 and S5 in Supporting Information S1) shows that this improvement is primarily due to one single-signed coarse-grained pattern along the coast that is amplified by the downscaling. While overall skill is notably lower on the East Coast, downscaling still improved skill there in a few areas, notably along the Northeast continental shelf and in a Southeast continental shelf region away from the coastline. Again, much of this improvement is dominated by one single-signed coastal pattern (Figures S4–S5 in Supporting Information S1). The effectiveness of the statistical downscaling method varies across the models (Figures S6–S11 in Supporting Information S1), with much more downscaling improvement for the CanCM3 and CanCM4 than the other models (see Long et al., 2021 for a skill analysis of the original hindcasts).

Figure 4 shows how downscaling improves the skill of hindcasts verified against tide gauge observations. Since tide gauge data were not assimilated into GLORYS, they provide an independent verification of our technique. For San Diego and San Francisco, downscaled hindcast skill is significantly improved compared to interpolated hindcast skill for almost all lead times. At lead-7 month, downscaling improves skill from 0.52 to 0.58 and 0.50 to 0.54 for these two stations respectively, which account for 22% and 20% of more variance explained. There is no significant improvement for South Beach except at lead-8 month. For the three stations on the East Coast (Figures 4d–4f), downscaled forecasts are significantly more skillful than interpolated forecasts for most lead times, with lead-7 improving from 0.12 to 0.21, 0.22 to 0.28, and 0.49 to 0.58 for Virginia Key, Charleston, and Atlantic City respectively. These improvements increase the variance explained from 1.4%, 4.8%, and 24% to 4.4%, 7.8%, and 33.6% respectively. The downscaled hindcasts also have reduced error magnitude than the interpolated hindcasts (Figure S12 in Supporting Information S1).

Long et al. (2021) noted that the model SSH hindcasts do not capture the observed trend in the Atlantic basin, largely due to their poor SSH initialization, which can have a pronounced impact on their coastal SSH skill. In contrast, the GLORYS data set does capture the trend, so therefore the downscaling operator could as well (Figures S3–S4 in Supporting Information S1). However, we found that detrending the GLORYS data did not notably change the downscaling operator (Figures S15–16 in Supporting Information S1) and therefore did not impact downscaled skill (Figures S13–14 in Supporting Information S1), that downscaling captures a structural

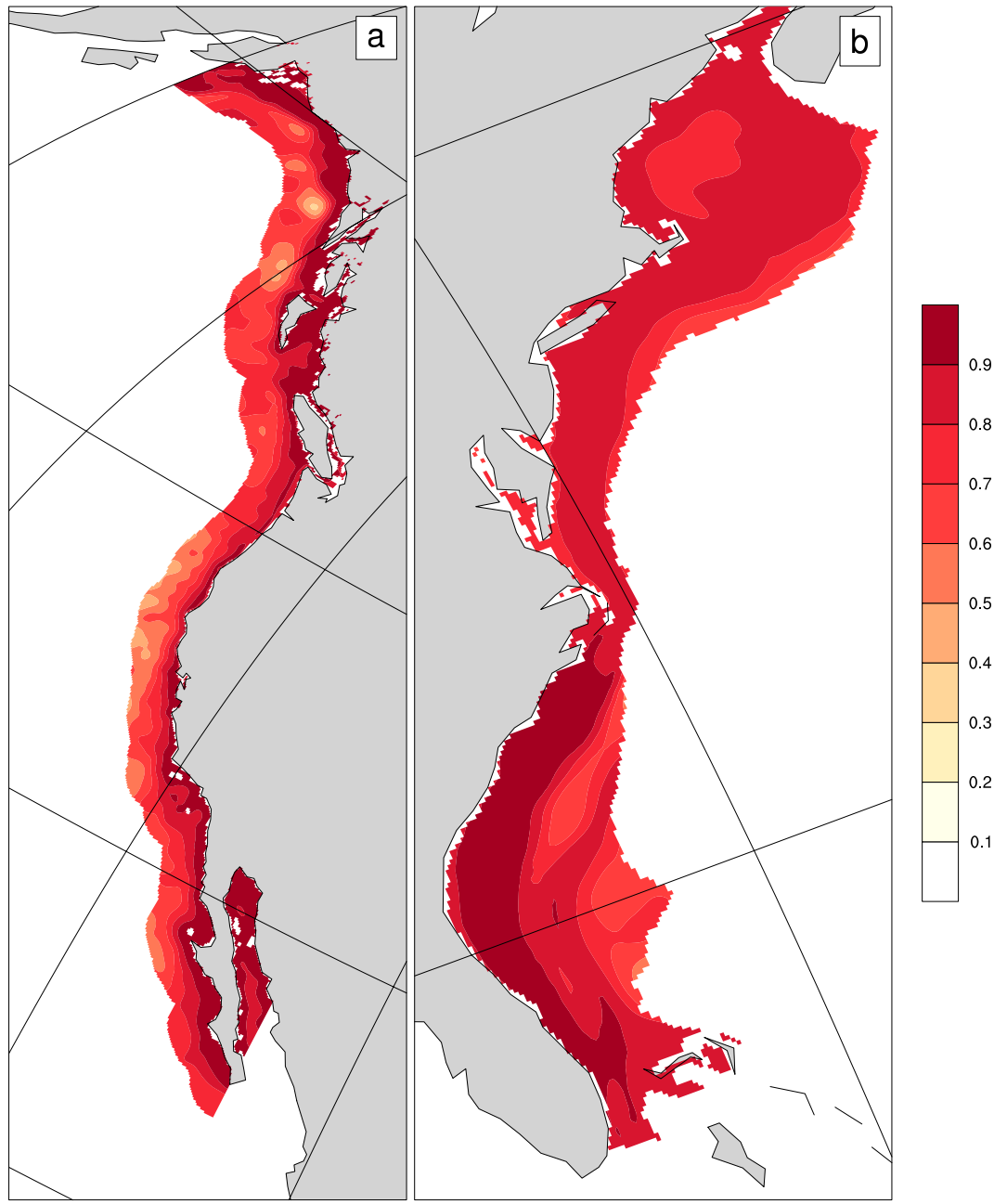

Figure 2. Temporal correlation coefficients between the sea surface height (SSH) anomalies from GLORYS and the regression predicted SSH anomalies for (a) West Coast and (b) East Coast.

relationship between large and fine scales that is not due to the trend. As expected, removing the linear trend in both the hindcast and tide gauge data sets also had very little impact on West Coast skill (Figure 4 and Figure S13 in Supporting Information S1). However, for the east coast tide gauges, downscaling primarily enhanced the local skill of the linear trend component (the single-signed coastal pattern in Figure S4 in Supporting Information S1). In fact, for the linearly detrended hindcasts, downscaling does not significantly improve east coast skill compared to simple interpolation (Figure S13 in Supporting Information S1).

SSH forecast skill has strong seasonality (Long et al., 2021) that typically depends on the verification month (Shin & Newman, 2021). Figure 5 shows the skill for each target month and lead time for San Diego and Charleston (other stations are in Figure S17 in Supporting Information S1). San Diego has higher skill for hindcasts

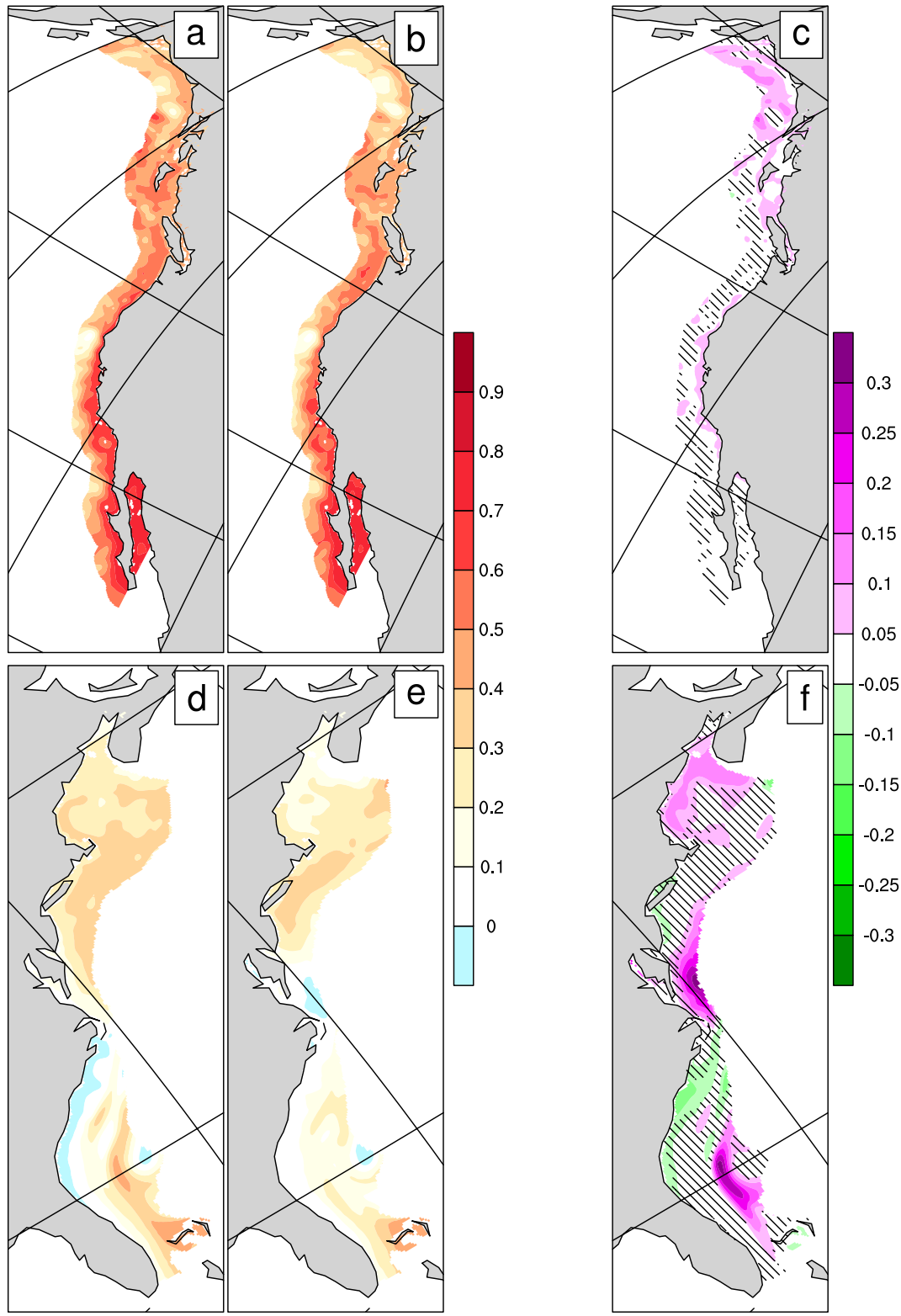

Figure 3. Hindcast skill (measured by anomaly correlation) for lead-7 month of (a, d) the downscaled hindcast and (b, e) the interpolated hindcast, verified against sea surface height anomaly from GLORYS reanalysis; (c, f) are the skill differences between downscaled and interpolated hindcasts; the hatching indicates where these differences are not statistically significant at 0.1 level.

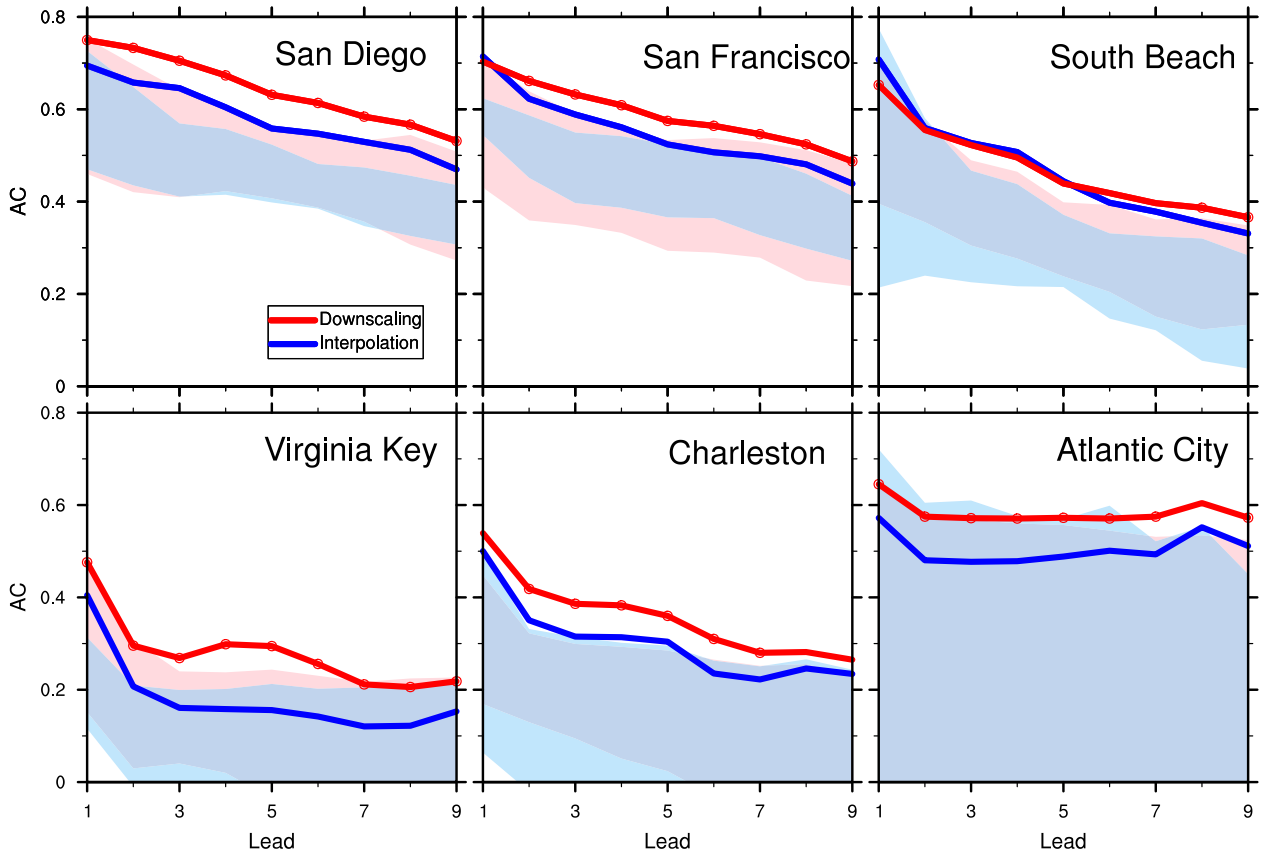

Figure 4. Hindcast skill (measured by anomaly correlation) of the downscaled (red) and interpolated (blue) hindcasts, verified against the tide gauge observations. The solid lines are the anomaly correlation of the respective ensemble mean of six models, and the shading indicates the skill range of all six models. The red circles indicate that the difference of skill between downscaled and interpolated hindcasts is statistically significant at that lead time at the 0.1 level.

verifying during the cold season, particularly October through February, consistent with a predictable signal due to ENSO-forced coastally trapped Kelvin Waves (Amaya et al., 2022). West coast sea level variability is also smaller in warm than in cold months. The skill of interpolated forecasts has similar seasonality. However, the seasonality of the skill is different than that of the skill difference. For example, statistical downscaling improves San Diego hindcast skill during both October–December and April–June. San Francisco and South Beach show similar seasonality of skill and skill difference as San Diego. In contrast, higher East Coast skill is found for hindcasts verifying during late summer and early autumn, for both downscaling and interpolation, which is also when the most significant downscaling skill improvement is found (Figure 5 and Figure S17 in Supporting Information S1). Note also that the downscaling leads to minimal skill improvement, or even minor skill degradation, during some winter months for most of the stations examined here.

5. Conclusion

In this study, we demonstrated that a downscaling operator, obtained by regressing fine-scale SSH anomalies onto coarse-grained SSH anomalies determined from a high-resolution reanalysis, can be applied to model forecasts to generate high-resolution seasonal forecasts of U.S. coastal SSH anomalies. We showed that our statistical downscaling technique significantly improved the hindcast skill of SSH anomalies for the U.S. coasts compared to bilinearly interpolated hindcasts. Specifically, when comparing the downscaled hindcasts to the selected six tide gauge observations, we found that the downscaled hindcasts improved skill for five stations at most lead times. This suggests that downscaling does capture some predictable fine-scale variations that are directly driven by predictable large-scale variations, which cannot be obtained by interpolation alone. Whether these improvements depended more on the resolution or on the quality of the GLORYS reanalysis data set used to construct the downscaling operators remains to be determined.

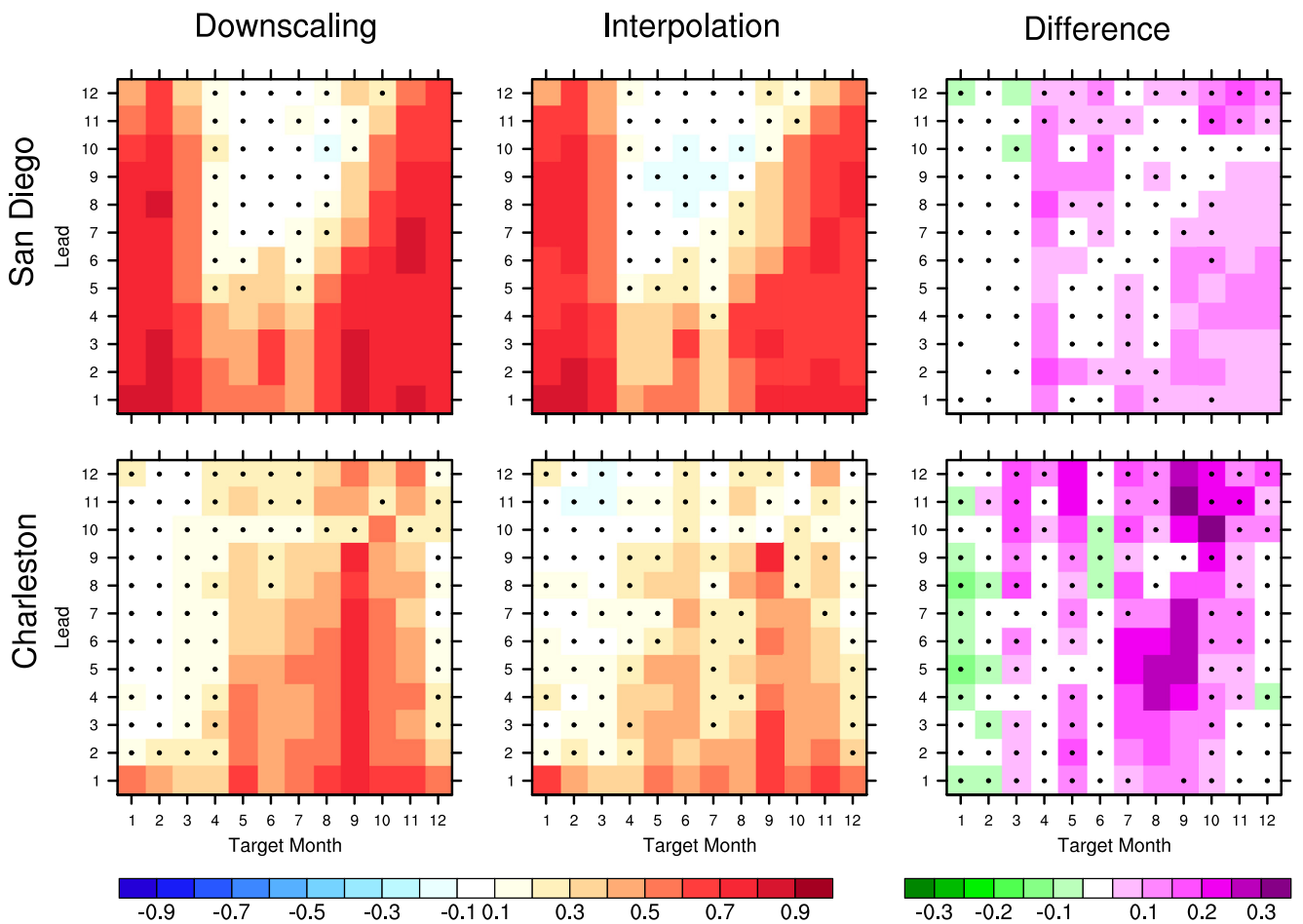

Figure 5. Hindcast skill (measured by anomaly correlation) of the ensemble mean of downscaled (left column) and interpolated (middle column) hindcasts, verified against the tide gauge observations at San Diego and Charleston, for each lead time and target month; the right column shows the skill differences between downscaled and interpolated hindcasts (downscaling minus interpolation). The black dots indicate the correlation or correlation difference is not statistically significant at that lead time and target month at the 0.1 level.

We did not aim to "correct" the hindcasts for model error, apart from removing the mean bias. That is, when the reanalysis-derived downscaling operator is applied to the model hindcasts it is assumed that the model space is largely similar to that of the reanalysis. Of course, models do not reproduce observed variability and their hindcasts may evolve in a different state space than nature (e.g., Ding et al., 2018), which may be why some model hindcasts are more improved than others by the downscaling. Applying a downscaling relationship determined entirely from observations to coarse-grained forecasts might therefore provide less high-resolution skill than a downscaling trained on the forecasts themselves, in which case it may also be useful to include other variables in the downscaling procedure, providing a focus for future work.

Data Availability Statement

The data used in this study are available from the following sources: tide gauge observations (https://psl.noaa.gov/data/tidal/), GLORYS reanalysis (https://datastore.cls.fr/catalogues/eu-copernicus-marine-service-global-reanalysis-glorys/) and retrospective forecasts (https://downloads.psl.noaa.gov/Projects/NMME/).

Acknowledgments
The authors thank the anonymous reviewers for their valuable comments that helped improve this study. The authors also thank the modeling centers for providing the seasonal forecast output. The authors acknowledge the support from NOAA cooperative agreements NA17OAR4320101 and NA22OAR4320151, and U.S. DoC/NOAA/Bipartisan Infrastructure Law (BIL).

References

Alexander, L. M. (1993). Large marine ecosystems: A new focus for marine resources management. *Marine Policy*, *17*(3), 186–198. https://doi.org/10.1016/0308-597x(93)90076-f

Alexander, M. A., Shin, S.-i., Scott, J. D., Curchitser, E., & Stock, C. (2020). The response of the northwest Atlantic Ocean to climate change. *Journal of Climate*, *33*(2), 405–428. https://doi.org/10.1175/jcli-d-19-0117.1

Allen, J. (1975). Coastal trapped waves in a stratified ocean. *Journal of Physical Oceanography*, *5*(2), 300–325. https://doi.org/10.1175/1520-0485(1975)005<0300:ctwias>2.0.co;2

Amaya, D. J., Jacox, M. G., Dias, J., Alexander, M. A., Karnauskas, K. B., Scott, J. D., & Gehne, M. (2022). Subseasonal-to-seasonal forecast skill in the California current system and its connection to coastal Kelvin waves. *Journal of Geophysical Research: Oceans*, *127*(1), e2021JC017892. https://doi.org/10.1029/2021JC017892

Anderson, T. R., Fletcher, C. H., Barbee, M. M., Frazer, L. N., & Romine, B. M. (2015). Doubling of coastal erosion under rising sea level by mid-century in Hawaii. *Natural Hazards*, *78*(1), 75–103. https://doi.org/10.1007/s11069-015-1698-6

Calafat, F. M., Wahl, T., Lindsten, F., Williams, J., & Frajka-Williams, E. (2018). Coherent modulation of the sea-level annual cycle in the United States by Atlantic Rossby waves. *Nature Communications*, *9*(1), 1–13. https://doi.org/10.1038/s41467-018-04898-y

Castro, C. L., Pielke, R. A., Sr., & Leoncini, G. (2005). Dynamical downscaling: Assessment of value retained and added using the regional atmospheric modeling system (RAMS). *Journal of Geophysical Research: Atmospheres*, *110*(D5), D05108. https://doi.org/10.1029/2004jd004721

Dahl, K. A., Fitzpatrick, M. F., & Spanger-Siegfried, E. (2017). Sea level rise drives increased tidal flooding frequency at tide gauges along the U.S. East and Gulf Coasts: Projections for 2030 and 2045. *PLoS One*, *12*(2), e0170949. https://doi.org/10.1371/journal.pone.0170949

Ding, H., Newman, M., Alexander, M. A., & Wittenberg, A. T. (2018). Skillful climate forecasts of the tropical Indo-Pacific Ocean using model-analogs. *Journal of Climate*, *31*(14), 5437–5459. https://doi.org/10.1175/jcli-d-17-0661.1

Ezer, T. (2016). Can the Gulf Stream induce coherent short-term fluctuations in sea level along the U.S. East Coast? A modeling study. *Ocean Dynamics*, *66*(2), 207–220. https://doi.org/10.1007/s10236-016-0928-0

Ezer, T., & Atkinson, L. P. (2014). Accelerated flooding along the U.S. East Coast: On the impact of sea-level rise, tides, storms, the Gulf Stream, and the North Atlantic oscillations. *Earth's Future*, *2*(8), 362–382. https://doi.org/10.1002/2014ef000252

Goubanova, K., Echevin, V., Dewitte, B., Codron, F., Takahashi, K., Terray, P., & Vrac, M. (2011). Statistical downscaling of sea-surface wind over the Peru-Chile upwelling region: Diagnosing the impact of climate change from the IPSL-CM4 model. *Climate Dynamics*, *36*(7), 1365–1378. https://doi.org/10.1007/s00382-010-0824-0

Habel, S., Fletcher, C. H., Anderson, T. R., & Thompson, P. R. (2020). Sea-level rise induced multi-mechanism flooding and contribution to urban infrastructure failure. *Scientific Reports*, *10*(1), 1–12. https://doi.org/10.1038/s41598-020-60762-4

Heyen, H., Zorita, E., & Von Storch, H. (1996). Statistical downscaling of monthly mean North Atlantic air-pressure to sea level anomalies in the Baltic sea. *Tellus*, *48*(2), 312–323. https://doi.org/10.3402/tellusa.v48i2.12062

Jean-Michel, L., Eric, G., Romain, B.-B., Gilles, G., Angélique, M., Marie, D., et al. (2021). The Copernicus global 1/12° oceanic and sea ice GLORYS12 reanalysis. *Frontiers of Earth Science*, *9*, 585. https://doi.org/10.3389/feart.2021.698876

Kirtman, B. P., Min, D., Infanti, J. M., Kinter, J. L., Paolino, D. A., Zhang, Q., et al. (2014). The North American Multimodel Ensemble: Phase-1 seasonal-to-interannual prediction; phase-2 toward developing intraseasonal prediction. *Bulletin of the American Meteorological Society*, *95*(4), 585–601. https://doi.org/10.1175/BAMS-D-12-00050.1

Klaver, R., Haarsma, R., Vidale, P. L., & Hazeleger, W. (2020). Effective resolution in high-resolution global atmospheric models for climate studies. *Atmospheric Science Letters*, *21*(4), e952. https://doi.org/10.1002/asl.952

Kriebel, D. L., Geiman, J. D., & Henderson, G. R. (2015). Future flood frequency under sea-level rise scenarios. *Journal of Coastal Research*, *31*(5), 1078–1083. https://doi.org/10.2112/jcoastres-d-13-00190.1

Kruel, S. (2016). The impacts of sea-level rise on tidal flooding in Boston, Massachusetts. *Journal of Coastal Research*, *32*(6), 1302–1309.

Little, C. M., Hu, A., Hughes, C. W., McCarthy, G. D., Piecuch, C. G., Ponte, R. M., & Thomas, M. D. (2019). The relationship between U.S. East Coast sea level and the Atlantic meridional overturning circulation: A review. *Journal of Geophysical Research: Oceans*, *124*(9), 6435–6458. https://doi.org/10.1029/2019jc015152

Long, X., Widlansky, M. J., Spillman, C. M., Kumar, A., Balmaseda, M., Thompson, P. R., et al. (2021). Seasonal forecasting skill of sea-level anomalies in a multi-model prediction framework. *Journal of Geophysical Research: Oceans*, *126*(6), e2020JC017060. https://doi.org/10.1029/2020JC017060

McIntosh, P. C., Church, J. A., Miles, E. R., Ridgway, K., & Spillman, C. M. (2015). Seasonal coastal sea level prediction using a dynamical model. *Geophysical Research Letters*, *42*(16), 6747–6753. https://doi.org/10.1002/2015gl065091

Merryfield, W. J., Lee, W.-S., Boer, G. J., Kharin, V. V., Scinocca, J. F., Flato, G. M., et al. (2013). The Canadian seasonal to interannual prediction system. Part I: Models and initialization. *Monthly Weather Review*, *141*(8), 2910–2945. https://doi.org/10.1175/mwr-d-12-00216.1

Meyers, S. D., Melsom, A., Mitchum, G. T., & O'Brien, J. J. (1998). Detection of the fast kelvin wave teleconnection due to El Niño-Southern Oscillation. *Journal of Geophysical Research: Oceans*, *103*(C12), 27655–27663. https://doi.org/10.1029/98jc02402

Miles, E. R., Spillman, C. M., Church, J. A., & McIntosh, P. C. (2014). Seasonal prediction of global sea level anomalies using an ocean-atmosphere dynamical model. *Climate Dynamics*, *43*(7), 2131–2145. https://doi.org/10.1007/s00382-013-2039-7

Moftakhari, H. R., AghaKouchak, A., Sanders, B. F., Feldman, D. L., Sweet, W., Matthew, R. A., & Luke, A. (2015). Increased nuisance flooding along the coasts of the United States due to sea level rise: Past and future. *Geophysical Research Letters*, *42*(22), 9846–9852. https://doi.org/10.1002/2015gl066072

Nerem, R. S., Beckley, B. D., Fasullo, J. T., Hamlington, B. D., Masters, D., & Mitchum, G. T. (2018). Climate-change-driven accelerated sea-level rise detected in the altimeter era. *Proceedings of the National Academy of Sciences*, *115*(9), 2022–2025. https://doi.org/10.1073/pnas.1717312115

Pasquet, S., Vilibić, I., & Šepić, J. (2013). A survey of strong high-frequency sea level oscillations along the U.S. East Coast between 2006 and 2011. *Natural Hazards and Earth System Sciences*, *13*(2), 473–482. https://doi.org/10.5194/nhess-13-473-2013

Piecuch, C. G., Huybers, P., Hay, C. C., Kemp, A. C., Little, C. M., Mitrovica, J. X., et al. (2018). Origin of spatial variation in U.S. East Coast sea level trends during 1900–2017. *Nature*, *564*(7736), 400–404. https://doi.org/10.1038/s41586-018-0787-6

Pielke, R. A.Sr., & Wilby, R. L. (2012). Regional climate downscaling: What's the point? *Eos Transactions—American Geophysical Union*, *93*(5), 52–53. https://doi.org/10.1029/2012eo050008

Rotzoll, K., & Fletcher, C. H. (2013). Assessment of groundwater inundation as a consequence of sea level rise. *Nature Climate Change*, *3*(5), 477–481. https://doi.org/10.1038/nclimate1725

Saha, S., Moorthi, S., Wu, X., Wang, J., Nadiga, S., Tripp, P., et al. (2014). The NCEP climate forecast system version 2. *Journal of Climate*, *27*(6), 2185–2208. https://doi.org/10.1175/jcli-d-12-00823.1

Sallenger, A. H., Doran, K. S., & Howd, P. A. (2012). Hotspot of accelerated sea level rise on the Atlantic coast of North America. *Nature Climate Change*, *2*(12), 884–888. https://doi.org/10.1038/nclimate1597

Shin, S.-I., & Alexander, M. A. (2020). Dynamical downscaling of future hydrographic changes over the northwest Atlantic Ocean. *Journal of Climate*, *33*(7), 2871–2890. https://doi.org/10.1175/jcli-d-19-0483.1

Shin, S.-I., & Newman, M. (2021). Seasonal predictability of global and North American coastal sea surface temperature and height anomalies. *Geophysical Research Letters*, *48*(10), e2020GL091886. https://doi.org/10.1029/2020gl091886

Sithara, S., Pramada, S., & Thampi, S. G. (2022). Statistical downscaling of sea levels: Application of multi-criteria analysis for selection of global climate models. *Environmental Monitoring and Assessment*, *194*(10), 1–21. https://doi.org/10.1007/s10661-022-10449-2

Smith, D. M., Eade, R., & Pohlmann, H. (2013). A comparison of full-field and anomaly initialization for seasonal to decadal climate prediction. *Climate Dynamics*, *41*(11), 3325–3338. https://doi.org/10.1007/s00382-013-1683-2

Soufflet, Y., Marchesiello, P., Lemarié, F., Jouanno, J., Capet, X., Debreu, L., & Benshila, R. (2016). On effective resolution in ocean models. *Ocean Modeling*, *98*, 36–50. https://doi.org/10.1016/j.ocemod.2015.12.004

Stammer, D. (1997). Global characteristics of ocean variability estimated from regional TOPEX/POSEIDON altimeter measurements. *Journal of Physical Oceanography*, *27*(8), 1743–1769. https://doi.org/10.1175/1520-0485(1997)027<1743:gcoove>2.0.co;2

Sweet, W., Park, J., Marra, J., Zervas, C., & Gill, S. (2014). *Sea level rise and nuisance flood frequency changes around the United States (Tech. Rep.)*. NOAA Technical Report NOS CO-OPS 073.

Thompson, P. R., Widlansky, M. J., Hamlington, B. D., Merrifield, M. A., Marra, J. J., Mitchum, G. T., & Sweet, W. (2021). Rapid increases and extreme months in projections of United States high-tide flooding. *Nature Climate Change*, *11*(7), 584–590. https://doi.org/10.1038/s41558-021-01077-8

Vannitsem, S., Wilks, D. S., & Messner, J. (2018). *Statistical postprocessing of ensemble forecasts*. Elsevier.

Vitousek, S., Barnard, P. L., Fletcher, C. H., Frazer, N., Erikson, L., & Storlazzi, C. D. (2017). Doubling of coastal flooding frequency within decades due to sea level rise. *Scientific Reports*, *7*(1), 1–9. https://doi.org/10.1038/s41598-017-01362-7

Wang, O., Lee, T., Piecuch, C. G., Fukumori, I., Fenty, I., Frederikse, T., et al. (2022). Local and remote forcing of interannual sea level variability at Nantucket Island. *Journal of Geophysical Research: Oceans*, *127*(6), e2021JC018275. https://doi.org/10.1029/2021jc018275

Wdowinski, S., Bray, R., Kirtman, B. P., & Wu, Z. (2016). Increasing flooding hazard in coastal communities due to rising sea level: Case study of Miami Beach, Florida. *Ocean & Coastal Management*, *126*, 1–8. https://doi.org/10.1016/j.ocecoaman.2016.03.002

Wedd, R., Alves, O., de Burgh-Day, C., Down, C., Griffiths, M., Hendon, H. H., et al. (2022). ACCESS-S2: The upgraded bureau of meteorology multi-week to seasonal prediction system. *Journal of Southern Hemisphere Earth Systems Science*, *72*(3), 218–242. https://doi.org/10.1071/es22026

Widlansky, M. J., Long, X., & Schloesser, F. (2020). Increase in sea level variability with ocean warming associated with the nonlinear thermal expansion of seawater. *Communications Earth & Environment*, *1*(1), 1–12. https://doi.org/10.1038/s43247-020-0008-8

Widlansky, M. J., Marra, J. J., Chowdhury, M. R., Stephens, S. A., Miles, E. R., Fauchereau, N., et al. (2017). Multimodel ensemble sea level forecasts for tropical Pacific Islands. *Journal of Applied Meteorology and Climatology*, *56*(4), 849–862. https://doi.org/10.1175/jamc-d-16-0284.1

Zhang, S., Harrison, M., Rosati, A., & Wittenberg, A. (2007). System design and evaluation of coupled ensemble data assimilation for global oceanic climate studies. *Monthly Weather Review*, *135*(10), 3541–3564. https://doi.org/10.1175/mwr3466.1